Hindawi
Advances in Civil Engineering
Volume 2023, Article ID 2977092, 13 pages
https://doi.org/10.1155/2023/2977092

Research Article

Dynamic and Static Multiobjective Topology Optimization for Gears of Directional Drill Transmission System

Xiaohong Zhao,[1,2] **Xianguo Yan**,[1] **Zhi Chen**,[1] **Linbo Li**,[3] **and Ruibin Ren**[3]

[1]*School of Mechanical Engineering, Taiyuan University of Science and Technology, Taiyuan 030024, China*
[2]*Fengtai Locomotive Depot, China Railway Beijing Bureau Group Co., Ltd., Beijing 100070, China*
[3]*Shanxi Jinding Gaobao Drilling Co., Ltd., Jincheng 048000, China*

Correspondence should be addressed to Xianguo Yan; yan_xg2008@126.com

Received 24 October 2022; Revised 14 December 2022; Accepted 15 December 2022; Published 10 January 2023

Academic Editor: Fabio Di Trapani

Copyright © 2023 Xiaohong Zhao et al. This is an open access article distributed under the Creative Commons Attribution License, which permits unrestricted use, distribution, and reproduction in any medium, provided the original work is properly cited.

Aiming at the multiobjective topology optimization design of the structure, this paper proposes a method to establish the comprehensive objective function based on the normalized subobjective of the compromise programming method and to determine the weight coefficient of the subobjective of the comprehensive objective function by the analytic hierarchy process (AHP). By using statistical analysis and modal analysis, the static and dynamic characteristics of the gear can be obtained. The single objective topology optimization is used to reduce the compliance of the gear and elevate the low-order natural frequency, and the frequency weighting method is used to suppress the oscillation phenomenon in the frequency-single-objective optimization. AHP was used to determine the weight coefficient of each subtarget. The compromise programming method is used for multiobjective topology optimization, and the gear design is improved according to the optimization results. By analyzing the improved gear structure, the weight of the optimized gear is reduced by 25.3%. The overall stiffness performance and strength performance are enhanced, and the natural frequencies of each order are improved to different degrees.

1. Introduction

Down hole, directional drilling technology is the key technology to control coal mine gas and ensure efficient extraction, and it is also one of the basic measures to ensure coal mine production safety [1]. A directional drill is equipment used for gas extraction, it drives the drill pipe by slewing device, and the drill pipe is connected with a bending joint to realize the drilling process. A slewing device is the core part of a drilling rig, which drives the drilling tool to turn and provides torque. It is primarily used to clamp the drill pipe, convert the speed and torque output from the hydraulic motor into those compatible with the drilling process requirements, transfer them to the the drill pipe to drive the slewing, and realize the omni–directional operation of the roadway [2–4]. In the process of drilling, the drill bit will produce a resistance moment when breaking rock, and the disturbance of the drill pipe and hole wall will also produce a resistance moment. All these external dynamic loads will act on the rotary, making it bear circumferential torsion and axial impact, which will affect the performance of the drill. At the same time, due to the narrow working environment characteristics of underground roadways in the coal mines, the drill must have a lighter weight and smaller volume to facilitate the installation and disassembly of the drill underground. Therefore, this paper optimizes the large gear at the output end of the gyrator to improve its static and dynamic characteristics and achieve the purpose of lightweighting and miniaturization.

Topology optimization is the most promising and innovative technique in structure optimization, which is to obtain the lightest design by finding the best material distribution or force transmission path in the design space. It is widely used in structural conceptual design [5, 6]. In the process of drilling, the external dynamic load will directly act on the helical gear at the output end of the rotary device. As

the output end of drilling power, the performance of the helical gear has a great influence on the rotary device to make the optimized gear not only meet certain mechanical characteristics but also have the ability to inhibit external excitation and at the same time achieve the purpose of being lightweight [7, 8]. In this paper, the multiobjective topology optimization method is adopted. The big gear at the output end of the gyrator is selected as the research object, the dynamic frequency characteristics and static stiffness characteristics of the gear are respectively taken as the optimization objectives for single objective optimization, and the compromise programming method is used to normalize each subobjective. The weight coefficients of each subobjective were determined by AHP, and the multiobjective topology optimization of gear was carried out [9, 10]. According to the optimization results, the web design of the gear is improved. The analysis results show that the improved gear strength performance and modal natural frequency are both improved, and the quality reduction effect is obvious. The topology optimization process is shown in Figure 1.

2. Topology Optimization Model

2.1. Material Interpolation Method. The variable density method is an efficient method for structural topology optimization, the continuum structure is discretized by the finite element method [11]. The corresponding relation between the relative density of the element and the elastic modulus of the material is expressed by the density interpolation function of the continuous variable. The relative density of each cell is taken as the optimization variable. In the optimization process, each element corresponds to an optimization variable. By changing the value of the optimization variable, the elastic modulus of the element in the structure changes, thus adjusting the change of the overall stiffness matrix of the structure and making the material layout in the structure tends to be optimal. There are two kinds of material interpolation models of the variable density method [12, 13]: solid isotropic material with penalization and rational approximation of material properties. Since the topology optimization problem based on density description is a discrete programming problem [14]. To solve the topology optimization problem efficiently, The discrete element density variable can be continuous, that is, ρ_i can take any value between 0 and 1. To avoid intermediate density elements in the optimization process, a penalty factor P is introduced, to avoid intermediate density elements in the optimization process, a penalty factor P is introduced to make the density value of the optimization result close to the original discrete variable and get a clear boundary, thus improving the quality of topology optimization [15, 16].

(1) Solid isotropic material with penalization:

$$E_i = \rho_i^P \cdot E_0 \, (i = 1, 2, \cdots, n). \tag{1}$$

(2) Rational approximation of material properties:

$$E(\rho_e) = \frac{\rho_e}{1 + q(1 - \rho_e)} E_0, \tag{2}$$

where E_i is the elastic modulus of the element i; P is the density penalty factor, generally taken as $P = 3$; ρ_i is the density of the element i; to avoid singular phenomena in the solution process, its value range is as follows: $0 \le \rho_{\min} \le \rho_e \le 1$, $\rho_{\min}$ is the density value of the void part; and E_0 is the elastic modulus of the part $\rho_i = 1$.

From a lot of engineering practices, the SIMP interpolation model is better than the RAMP interpolation model, so this paper chooses the SIMP interpolation model for optimization design.

2.2. The Topology Optimization Algorithm. Optistruct uses three methods to build approximate models: Paired method, Feasible direction method and the optimization criterion method. The optimization criterion method is applied to solve the classical topology optimization problem. The optimization steps of the optimization criterion method are as follows: Start with an initial design $x^{(k)}$, k is the number of iterations, this method does not need to consider the constraint conditions and the state of the objective function, as long as the optimal computing conditions for each iteration are achieved, then an improved design $x^{(k+1)}$ can be calculated, its iterative formula can be expressed as follows:

$$x^{(k+1)} = C^{(k)} x^{(k)}. \tag{3}$$

The advantage of the optimization criterion method is that it is simple, has small computation, has clear physical meaning, fast iteration convergence speed, and structure reanalysis fewer times.

2.3. Finite Element Model of Gear. The reducer transmission system uses a double planetary deceleration and helical gear deceleration combined with a two-stage deceleration type. The gear transmission structure of the rotary reducer is shown in Figure 2. The transmission system is a two-stage deceleration. The first stage of deceleration has two NGW-type planetary gear trains with the same structure. NGW is shorthand for a planetary array structure (N for internal engagement, G for a common planetary wheel, and W for a external engagement). Each planetary gear train comprises a sun gear A, a planetary wheel C, an inner ring B, and a planetary frame X. The inner gear ring is fixed, the central wheel is the input end, the planetary rack is the output end, and the number of planetary wheels is four. The second stage of deceleration is a helical gear set driven by a planetary frame. The helical gear set comprises a small helical gear D and a large helical gear E.

The large helical gear E is taken as the research object, and the gear material is 20CrNi4. The material properties and geometric parameters are shown in Table 1.

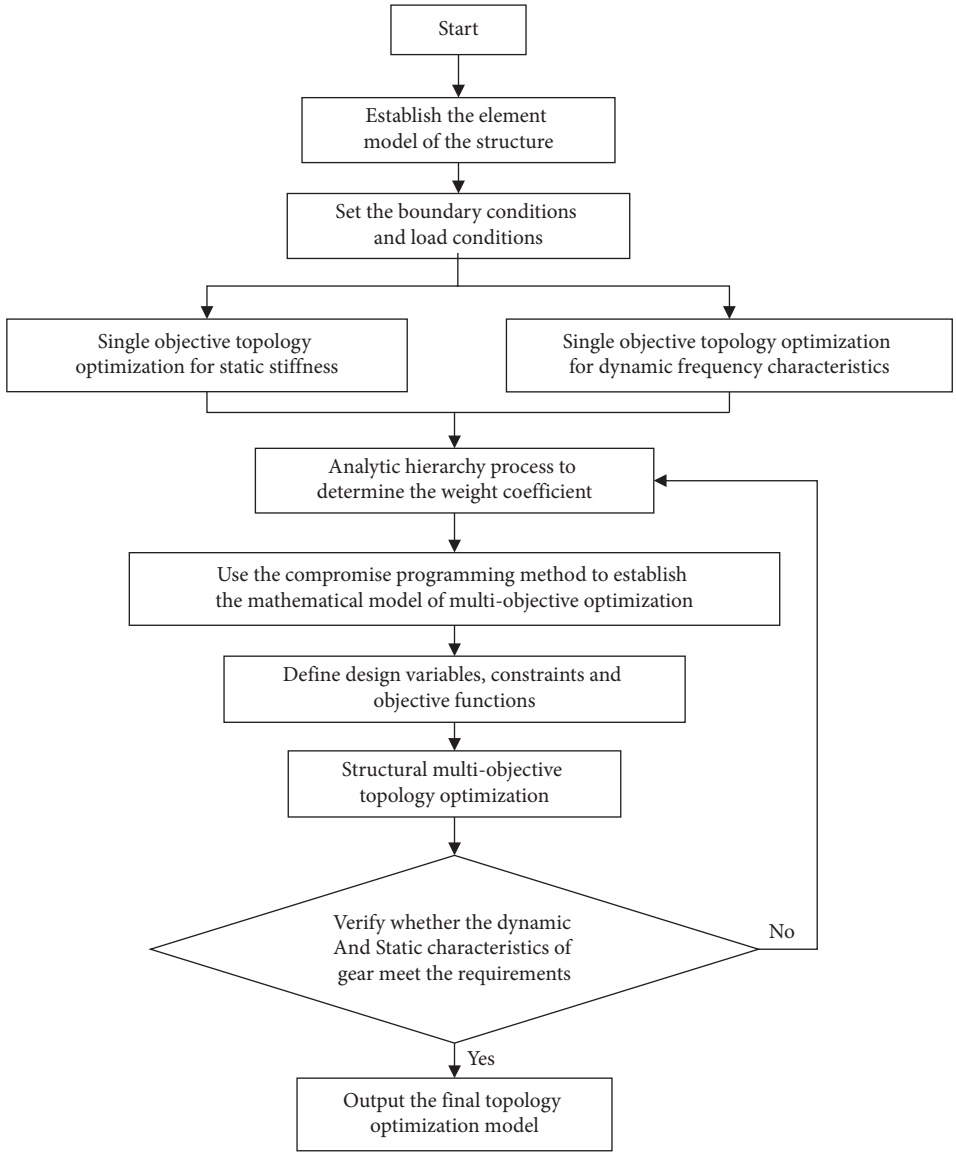

Figure 1: Schematic of the topology optimization process.

The 3D solid model of the gear is imported into Hypermesh, and the hexahedral mesh of the gear is divided. Gears are divided into design area and nondesign area, and the gears are given material property and P_{solid} property. The gear holes are connected with the main shaft by keys, create a node in the center of the gear, and connect all the nodes of the inner ring with the central node by RBE2 rigid unit to create coupling constraints. The boundary condition is to constrain the five degrees of freedom, only releasing the them around the axis of rotation. In the statics analysis, a fixed constraint is added near the pitch line of two gears 12 apart to simulate the force of gear meshing. According to the transmission diagram and force situation of the gear, the helical gear E is subjected to a circular force of 503.28 N applied by two small helical gears at the meshing place, and the output torque of the gear center is 7200 Nm. The finite element model of gear is shown in Figure 3.

3. Single Objective Topology Optimization of Gears

3.1. Topology Optimization Based on Static Stiffness Characteristics. Structural compliance reflects the strain capacity of the structure, which can be expressed by the strain energy stored in the structure or the work done by external forces in the process of structural deformation. Under the action of external force, the structural flexibility is equal to the reciprocal of the stiffness; that is, the larger the structural stiffness, the smaller the structural flexibility [17]. To control the maximum deformation of gear, overall structural compliance is adopted as the optimization objective [18]. Taking unit material density value ρ_i as the design variable, the minimum compliance is taken as the optimization objective, and the volume ratio before and after optimization is taken as the constraint condition. The

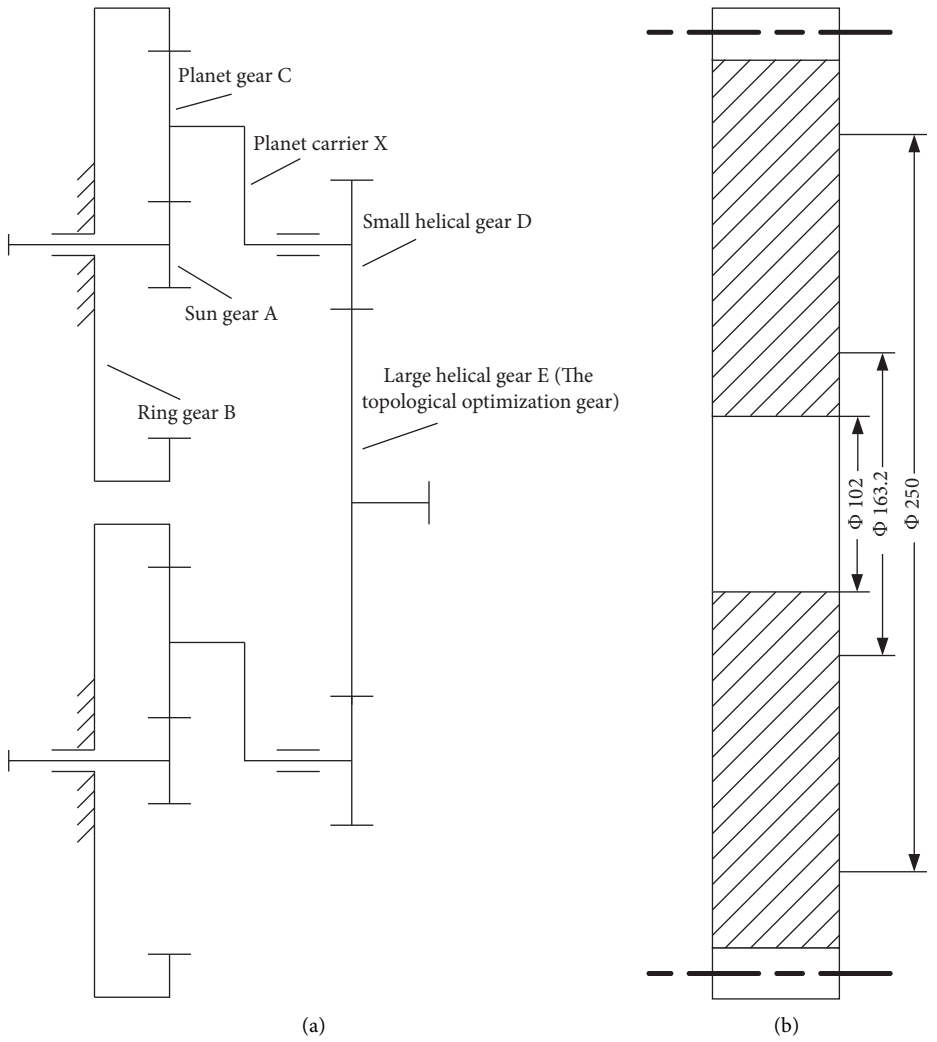

Figure 2: Schematic of the rotary transmission system. (a) Schematic of the transmission system. (b) Structure schematic of the large helical gear.

Table 1: The gear parameter.

Property	Numerical value
Young's modulus (Pa)	$2.07E+11$
Poisson's ratio	0.29
Density (kg/m^3)	7800
Helix angle	8°
Tooth width b (mm)	60
Number of teeth z	65
Normal modulus m_n (mm)	5
Reference diameter (mm)	328.28

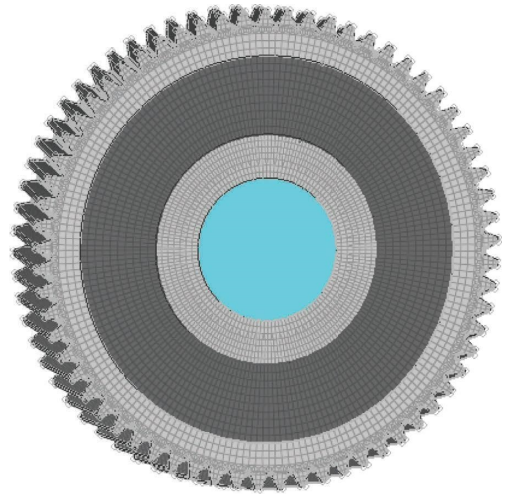

Figure 3: Schematic of a gear finite element model.

optimization model of the solid isotropic material penalty method for gear is expressed as follows [19]:

$$\begin{cases} \text{find } x = (x_1, x_2, x_3, \cdots, x_n)^T \in R, \\ \min C(x) = \{U\}^T [K]\{U\}, \\ \text{s.t.} \sum_{j=1}^{n} v_j x_j - v = 0, 0 < x_{\min} \le x_i \le x_{\max} \le 1, \\ i = 1, 2, \cdots, l, j = 1, 2, \cdots, n, \end{cases} \tag{4}$$

where x is the unit variable; n is the total number of units; C is structural compliance; $[K]$ represents the system stiffness matrix; $\{U\}$ represents the displacement vector of the structure; v is the volume constraint; $x_{\min}$ is the lower limit of design variables; and $x_{\max}$ is the upper limit of design variables.

Import the 3D model of gear into Hypermesh, the gear was meshed by hexahedron, and the material attribute and P_{solid} attribute were given to the gear. The gear is divided into a design area and a nondesign area and created a node in the center of the gear. All the nodes of the inner ring are connected with the central node by RBE2 rigid unit to create coupling constraints. A fixed constraint is added to the contact surface of two gears with 12 adjacent teeth to simulate the force of gears during meshing [20]. The load condition is to add $T = 7200\text{N} \cdot \text{m}$ torque at the center node. The boundary constraint is to release only the degree of freedom about the rotation axis.

Firstly, the gear is analyzed statically. The Von Mises stress and displacement cloud diagram of gear can be obtained, as shown in Figure 4. According to the figure, the maximum stress of the gear appears on the meshing line of the gear, and the stress value is 263.9 MPa. The maximum displacement is 0.09428 mm. Based on the statics analysis, the material element density value is created as the topology optimization variable. To control the occurrence of the checkerboard phenomenon during the optimization process, the minimum cell size is controlled to be 2–3 times the average grid size, and axial symmetric manufacturing constraints are added [19]. The constraint condition is that the volume ratio before and after optimization is ≤50%. Take compliance minimization as the design objective to conduct topology optimization, and obtain topology optimization results, as shown in Figure 5. Figure 6 shows the compliance iteration process of static topology optimization. It can be seen from the figure that the maximum value of gear compliance is 1.377 mm/N and the minimum value is 1.210 mm/N.

3.2. Topology Optimization Based on Dynamic Frequency Characteristics. Because the low-order natural frequency of the structure is close to the external excitation, it is easy to cause the gear resonance phenomenon. The topology optimization of dynamic frequency characteristics is aimed at improving the low-order frequency. In modal single objective optimization, the optimization process of each order frequency is not a positive correlation, which may occur when the frequency of one order is maximum, other times frequency will have a larger lower phenomenon, which can appear even the frequency switching between different orders, thus cause the iterative oscillation of the objective function, so that the optimization process is difficult to converge [10]. To solve this problem, make the lower order frequency relatively best on the whole. The average frequency method is introduced. The more the average frequency participates in the order, the more obvious the effect of reducing the iterative oscillation is [21]. However, the optimized frequency value may be less than that of direct single-objective optimization. The optimization objective is to maximize the average frequency of the first six orders. To obtain the maximum value of the average frequency and improve the low-order frequency at the same time, the weight values of each order frequency are 0.3, 0.3, 0.2, 0.2, 0.1, and 0.1. Taking the unit material density value ρ_i as the design variable, the volume ratio before and after optimization is taken as the constraint condition. The gear dynamic frequency topology optimization model is expressed as follows:

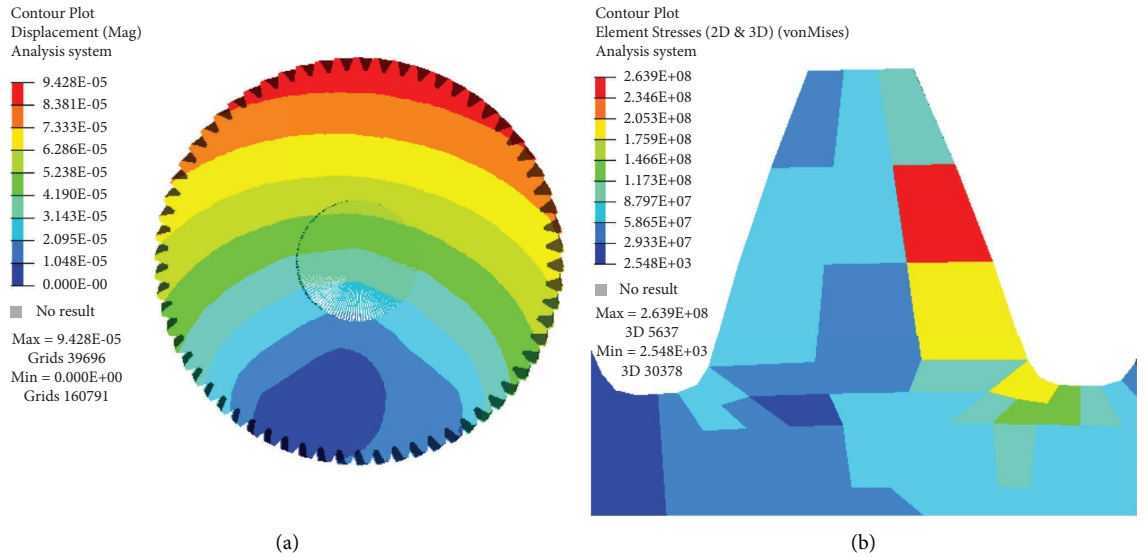

Figure 4: Schematic of gear statics analysis results. (a) Schematic of gear displacement cloud. (b) Schematic of gear Von Mises stress cloud.

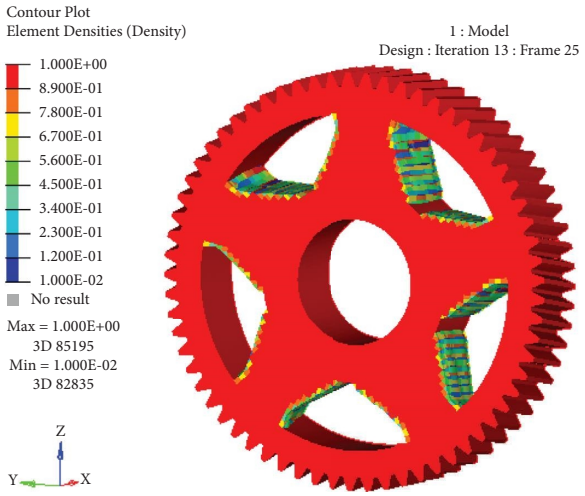

Figure 5: Schematic of static topology optimization results.

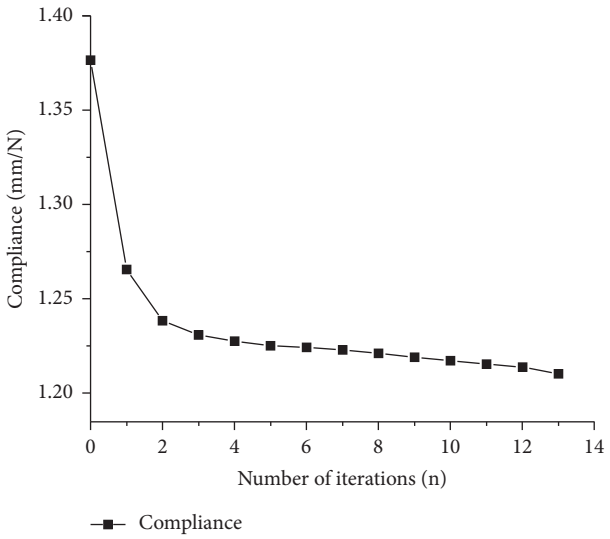

Figure 6: Schematic of the compliance iteration process.

$$\begin{cases} \text{find } x = (x_1, x_2, x_3, \cdots, x_n)^T \in R, \\ \max \Lambda(x) = \lambda_0 + \alpha \left(\sum_{k=1}^{m} \dfrac{w_k}{\lambda_k - \lambda_0} \right)^{-1}, \\ \text{s.t.} \sum_{j=1}^{n} v_j x_j - v = 0, 0 < x_{\min} \le x_i \le x_{\max} \le 1, \\ k = 1, 2, \cdots, m, j = 1, 2, \cdots, n, \end{cases} \tag{5}$$

where $\Lambda(x)$ is the average eigenvalue; λ_0, α is the given parameter, used to adjust the objective function; m is the order of eigenvalues to be optimized; w_k is the weight coefficient of k-order eigenvalues; and λ_k is an eigenvalue of order k.

Preprocessing is similar to static topology optimization, the gear was meshed by a hexahedron, and the material attribute and P_{solid} attribute were given to the gear, creating a node in the center of the gear. All the nodes of the inner ring are connected with the central node by the RBE2 rigid unit to create coupling constraints. Firstly, the modal analysis of the gear was carried out to obtain the first six-order frequency values of the gear, as shown in Table 2. Based on the modal analysis, the material element density value is created as the topology optimization variable. To control the occurrence of the checkerboard phenomenon during the optimization process, the minimum cell size is controlled to be 2–3 times the average grid size, and axial symmetric manufacturing constraints are added. The constraint condition is that the volume ratio before and after optimization is ≤50%. The optimization objective is the maximum value of the average frequency of the first six orders. After solving, the dynamic topology optimization result of gear structure can be obtained, as shown in Figure 7.

The iteration process is shown in Figure 8. It can be seen from the figure that the objective function converges after 28 iterations. The first six frequency iterations are shown in Figure 9, After optimization, the first and second-order natural frequencies are increased to 2309.015 Hz, the third-order frequency is reduced to 2399.557 Hz, the fourth-order frequency is increased to 2684.151 Hz, and the fifth and sixth-order frequencies are increased to 2804.088 Hz. The frequency of each order oscillates slightly in the iteration, but the changing trend is stable in the late iteration, and there is no alternating oscillation phenomenon in the first six order frequencies. Because the gear has a symmetric structure, the first-order frequency value is equal to the second-order frequency value, and the fifth-order frequency value is equal to the sixth-order frequency value.

Table 2: Gear modal analysis results.

Order	Natural frequency (Hz)
1	2268.65
2	2268.65
3	2422.38
4	2611.66
5	2611.66
6	2635.52

4. Multiobjective Topology Optimization Based on AHP

4.1. Topology Optimization Model and Weight Coefficient. Because the single-objective topology optimization of gear considers few factors. It is difficult to meet the actual engineering needs to make the gear structure have good mechanical properties, the static stiffness characteristics and dynamic frequency characteristics should be considered in the topology optimization stage. Therefore, multiobjective topology optimization of gears is carried out in this paper. Due to the different properties of stiffness and frequency, the numerical difference is obvious. The stiffness values and deformation modes of different working conditions are very different, and the frequency values of different orders are also obviously different, so it is difficult to achieve the optimal solution at the same time. Therefore, when the multiobjective optimization problem is transformed into a single objective optimization problem, it is necessary to normalize each subobjective [10, 22, 23]. In this paper, the compromise programming method with weight coefficients is used to deal with multiobjective optimization problems, and the comprehensive objective function is expressed as follows:

$$\begin{cases} \min F(x) = \left[w^2 \left(\sum_{i=1}^{l} w_i \dfrac{C_i^{\max} - C_i(x)}{C_i^{\max} - C_i^{\min}} \right)^2 + (1-w)^2 \left(\dfrac{\Lambda_i^{\max} - \Lambda_i(x)}{\Lambda_i^{\max} - \Lambda_i^{\min}} \right)^2 \right]^{1/2}, \\ \text{s.t.} \sum_{j=1}^{n} v_j x_j - v = 0, \beta(y) \geq \beta^*, \\ 0 < x_{\min} \leq x_i \leq x_{\max} \leq 1, \quad i = 1, 2, \cdots, n, \end{cases} \tag{6}$$

where l is the load condition; w_i is the weight coefficient of i-order eigenvalues; x_j is the density of the j the element; $C_i(x)$ is the compliance value of working condition k; $C_i^{\max}$ and $C_i^{\min}$ are the maximum and minimum compliance values of working condition k; $\Lambda_i^{\max}$ and $\Lambda_i^{\min}$ are the maximum and minimum values of the frequency objective function, and w_k is the weight value of each subtarget.

When the compromise programming method is used to solve the multiobjective topology optimization problem, the corresponding weight of each optimization objective should be found [24]. According to the paper [25], the scheme of AHP to determine the weight coefficient has higher computational efficiency in topology optimization design, and the generated topology structure is more detailed, the force transmission path is more reasonable, and the stability is better. So this paper uses the AHP to determine the weight of each target. The basic idea of AHP is to decompose decision-making-related elements into goals, criteria, schemes, and other levels and then conduct quantitative analysis [26]. The AHP builds the decision layer of the problem to be evaluated. Then, according to the paired comparison method, the importance degree of each subobjective is obtained by pairwise comparison. Constructing decisions matrix $W = (W_{ij})_{n\times n}$, n represents the number of subtargets, W_{ij} is the importance of the paired comparison between decision level i and decision level j [27]. The decision matrix is expressed as follows:

$$W = \begin{pmatrix} W_{11} & W_{12} & \cdots & W_{1n} \\ W_{21} & W_{22} & \cdots & W_{2n} \\ \vdots & \vdots & & \vdots \\ W_{n1} & W_{n2} & \cdots & W_{nn} \end{pmatrix}. \tag{7}$$

The eigenvector of the decision matrix is the weight ratio of each working condition in the integrated objective function. To transform the decision level comparison into a numerical comparison, the initial importance reference definition is given, as shown in Table 3.

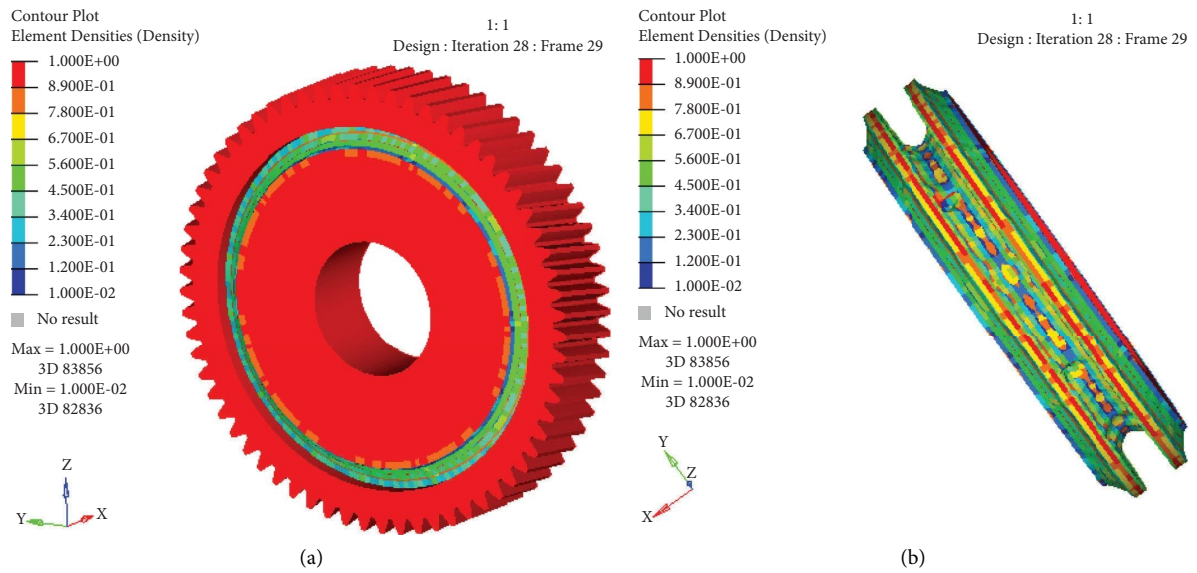

Figure 7: Schematic of gear dynamic topology optimization results. (a) Schematic of topology optimization results. (b) Schematic of design area optimization results.

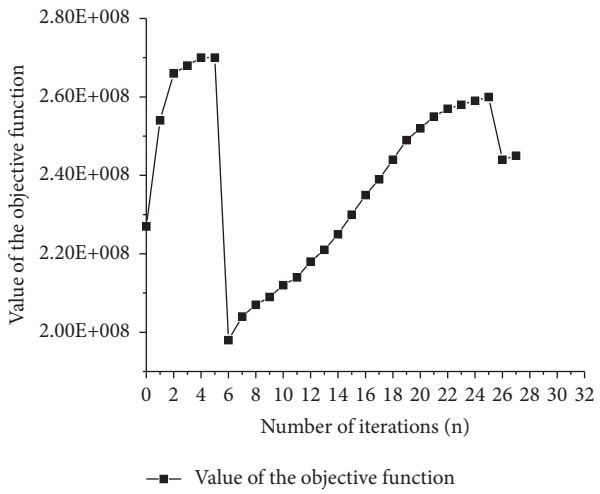

Figure 8: Schematic of gear dynamic topology optimization iteration process.

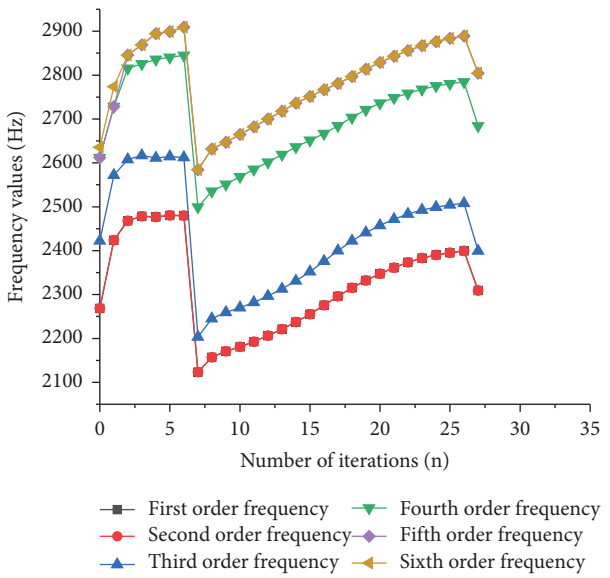

Figure 9: Schematic of the first six-order frequency iteration process of gear dynamic topology optimization.

In practice, the pairing decision matrix given by the designer is generally inconsistent. If the number of nonzero eigenvectors of the matrix is greater than 1, it is necessary to determine which eigenvector represents the desired weight ratio vector. Therefore, the prerequisite is to ensure the consistency of the pairing matrix. If the consistency requirements are not met, the pairing matrix needs to be reestablished [28]. The consistency ratio (CR) can be used to judge the consistency degree of each pairing matrix [29]. If the consistency ratio is satisfied,

$$\mathrm{CR} = \frac{\mathrm{CI}}{\mathrm{RI}} < 0.1, \tag{8}$$

then the consistency is acceptable.

Where CI—coincident indicator, $\mathrm{CI} = (\lambda_{\max} - n)/(n-1)$, $\lambda_{\max}$—The largest eigenvalue of the matrix; RI—randomly generated matrix consistency index.

Therefore, the decision matrix of gear multi-objective optimization is expressed as follows:

$$W = \begin{pmatrix} W_{11} & W_{12} \\ W_{21} & W_{22} \end{pmatrix}, \tag{9}$$

where W_{11}, W_{12}—the relevant elements of the objective function of static compliance; W_{21}, W_{22}—the relevant elements of the objective function of modal natural frequency;

Table 3: The definition of the importance scale of the judgment matrix.

Importance Degree	Ratio of importance W_{ij}
i is equally important with j	1
i is slightly more important than j	3
i is more important than j	5
i is far more important than j	7
i is significantly more important than j	9
j is slightly more important than i	1/3
j is more important than i	1/5
j is far more important than i	1/7
j is significantly more important than i	1/9

Define diagonal elements according to analytic hierarchy process $W_{11} = W_{22} = 1$

Because the gear needs a certain stiffness to determine the stability of the transmission, the dynamic characteristics are more important. According to the AHP, the decision matrix is parameterized as follows:

$$W = \begin{pmatrix} 1 & \frac{1}{3} \\ 3 & 1 \end{pmatrix}. \tag{10}$$

By solving the decision matrix, it can be known that the maximum eigenvalue is $\lambda_{W\max} = 2$, the eigenvector is $P = \begin{pmatrix} 1 \\ 3 \end{pmatrix}$. By verification, the matrix meets the consistency requirements. Therefore, the weight coefficients of each optimization objective of multi-objective topology optimization are 0.25 and 0.75.

4.2. Topology Optimization Process and Results. Due to the limitation of OptiStruct, only a single objective function optimization design can be carried out, especially in non-convex optimization problems that cannot get all Pareto solutions. Use the equation function definition panel in Optistruct, according to the maximum and minimum values of compliance and average frequency in single objective topology optimization, based on the multiobjective optimization formula, and using the sum of residual squares, the objective function is defined as follows:

$$F(x1, x2) = rss\left[\frac{0.25\,(x1 - 1.20395)}{0.17256}, \frac{0.75\,(284864000 - x2)}{71297000}\right], \tag{11}$$

where $x1$ is the compliance value of static topology optimization, and $x2$ is the frequency value of dynamic topology optimization.

The preprocessing settings of multiobjective optimization are consistent with those of single-objective extension optimization. The material element density value is created as the topology optimization variable. To control the occurrence of the checkerboard phenomenon during the optimization process, the minimum cell size is controlled to be 2–3 times the average grid size, and axial symmetric manufacturing constraints are added. The constraint condition is that the volume ratio before and after optimization is ≤50%. The optimization objective is to find the minimum value of the objective function. By solving, the multiobjective topology optimization results of gear structure can be obtained, as shown in Figures 10–14.

Figure 11 shows that the objective function converges after 10 steps of iteration. It can be seen from Figures 12–14, after multiobjective topology optimization, the low-order natural frequency of gear increases, and the compliance value decreases from 1.348 N·mm to 1.225 N·mm. The statistical analysis of the optimized gear is carried out. The cloud image of the gear is obtained, as shown in Figure 13, the maximum stress of the gear appears on the meshing line of the gear, and the stress value is 264 MPa, and the maximum displacement is 0.07763 mm. The compliance and frequency are mutually restricted. From the fourth iteration, the frequency value first decreases and then suddenly increases, and the flexibility value first increases and then suddenly decreases. This is because Optistruct uses the SIMP material interpolation model in its optimization process to obtain a more discrete structure, the minimum member size is set in the optimization. In the initial stage of optimization, the penalty coefficient $\rho = 2$, with the progress of optimization, the penalty coefficient increases to $\rho = 3$. Because there are intermediate density elements in the optimization process, a jump will occur for the objective function when ρ is increased by 1, which can be observed in Figures 12 and 14 [30]. There is a slight oscillation phenomenon in each order frequency during the iteration process, but the changing trend is stable in the late iteration, and there is no alternating oscillation phenomenon in the first six order frequencies, which proves that the optimization is feasible. Because the gear has a symmetric structure, the first-order frequency

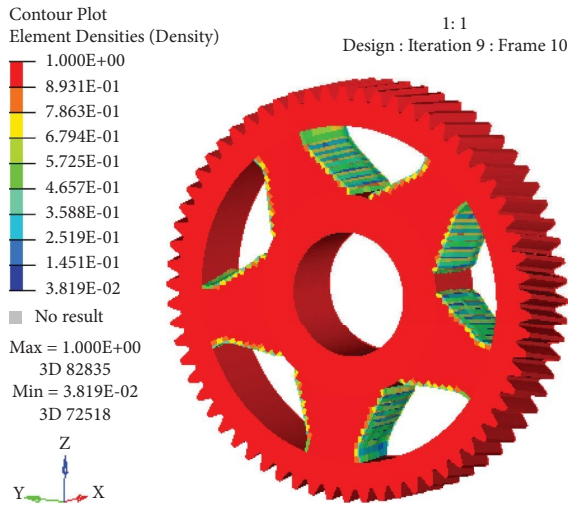

Figure 10: Schematic of the results of multiobjective topology optimization.

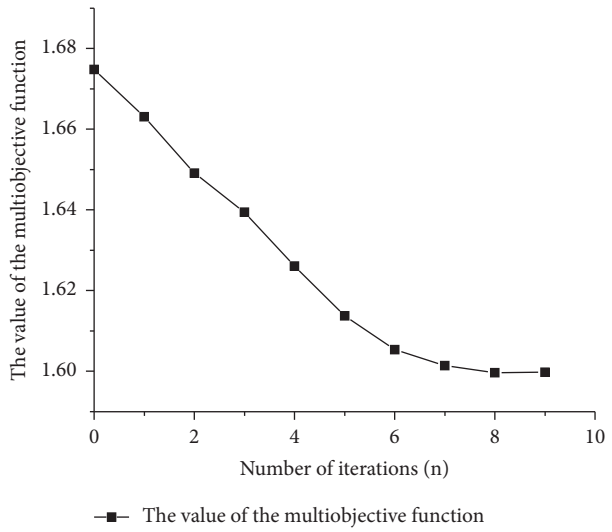

Figure 11: Schematic of the iterative process of multiobjective optimization.

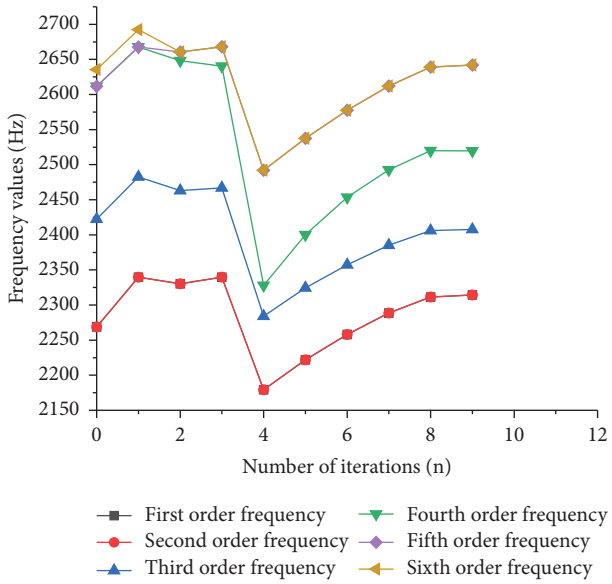

Figure 12: Schematic of the first six-order frequency iteration process of multiobjective optimization.

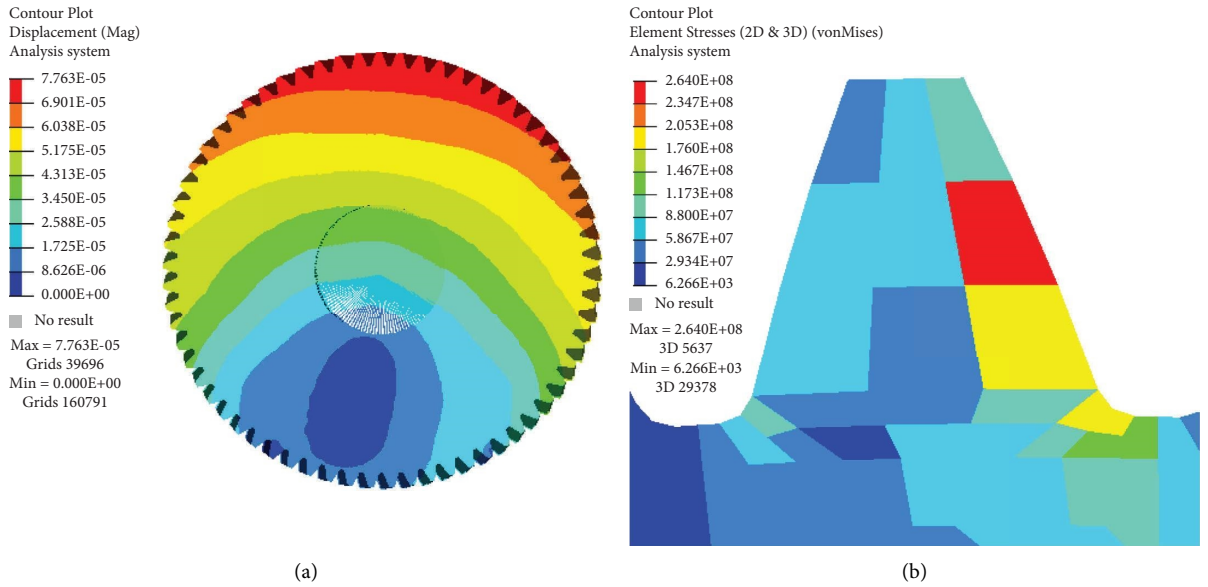

Figure 13: Statics analysis of a multiobjective optimization model. (a) Schematic of gear displacement cloud. (b) Schematic of gear Von Mises stress cloud.

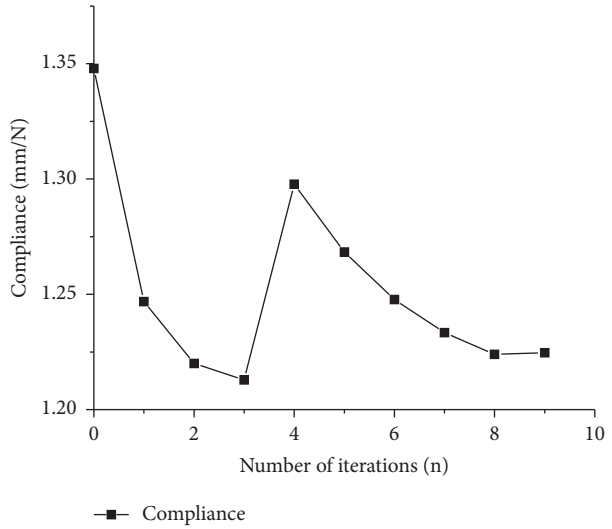

Figure 14: Schematic of the compliance iterative course of multiobjective optimization.

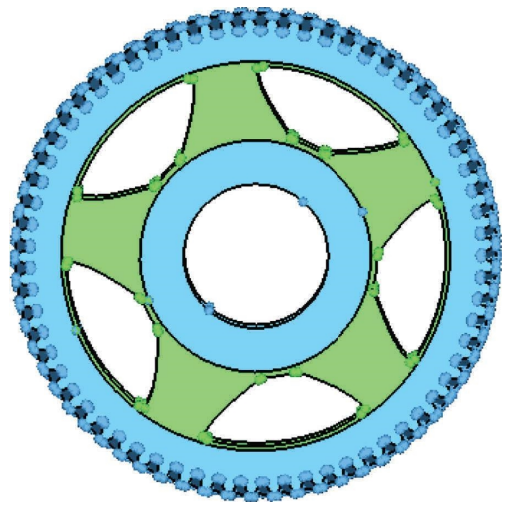

Figure 15: Schematic diagram of the improved gear structure.

Table 4: Comparison of gear performance before and after multiobjective optimization.

Subunit objectives	Before optimization	After optimization	Variable quantity (%)
Maximum deflection (mm)	0.094	0.078	−17
Maximum stress (MPa)	263.9	264	0.04
The first-order natural frequencies (Hz)	2268.65	2314.39	2.02
The second-order natural frequencies (Hz)	2268.65	2314.39	2.02
The third-order natural frequencies (Hz)	2422.38	2407.74	−0.6
The fourth-order natural frequencies (Hz)	2611.66	2519.51	−3.53
The fifth-order natural frequencies (Hz)	2611.66	2642.02	1.06
The sixth-order natural frequencies (Hz)	2635.52	2642.02	0.25
Mass (kg)	36.069	26.9428	−25.3

value is equal to the second-order frequency value, and the fifth-order frequency value is equal to the sixth-order frequency value.

Therefore, a jump will occur for the objective function when q is increased by 1, which can be observed in Figures 8 and 9.

4.3. Model Reconstruction. The material density distribution cloud image after multi-objective topology optimization is used as the basis for improving the design. In Hypermesh, the geometry is extracted through OSSmooth in the post-panel and the gears are remodeled taking into account the processing conditions of the structure, as shown in Figure 15. Static analysis and modal analysis of the improved gear are carried out, and the analysis results are shown in Table 4.

The weight of the improved gear is 26.9482 kg, which is 25.3% less than that of the original structure. Static and modal analysis of the improved gear is carried out, and the results are shown in Table 4. The deformation of the modified gear structure is reduced from 0.09428 mm to 0.07763 mm, the stiffness performance is improved, the first six natural frequencies are slightly reduced in the third and fourth orders, and the other four orders are increased to varying degrees, and the dynamic characteristics are significantly improved.

5. Conclusion

(1) Topology and multiobjective theory are adopted to optimize the structure design of the large gear in the transmission system of the directional drilling rig, considering the dynamic and static characteristics of the gear, By combining the compromise programming method with the analytic hierarchy process (AHP), an optimization method was proposed, which used the compromise programming method to normalize the subobjectives and determined the weight coefficients of subobjectives through the hierarchical analysis. OptiStruct was used to optimize the multiobjective topology of the gear.

(2) To reduce the frequency altercation and oscillation phenomenon IN the process of natural frequency subobjective optimization of gear, a new objective function is obtained by using the weighted average frequency method, which makes the iteration of natural frequency subobjective optimization tends to be stable, the convergence speed is faster, the optimization effect is better. The optimized gear model is reconstructed, and its static and dynamic analysis is carried out. The analysis results show that the stiffness performance of the gear is significantly enhanced, the first six natural frequencies are improved to varying degrees, and the weight reduction effect is obvious, which also provides a theoretical basis for the lightweight design of other structures.

Data Availability

The data used to support the findings of this work are included in the article.

Conflicts of Interest

The authors declare that there are no conflicts of interest.

Acknowledgments

This work was supported by the Key Research and Development Program of Shanxi Province (Grant no. 202003D111008).

References

[1] H. Wang, E. Wang, Z. Li, R. Shen, and X. Liu, "Study and application of a new gas pressure inversion model in coal seam while drilling based on directional drilling technology," *Fuel*, vol. 306, Article ID 121679, 2021.

[2] Y. Ningping, Z. Jie, J. Xing, and H. Hanjing, "Status and development of directional drilling technology in coal mine," *Procedia Engineering*, vol. 73, pp. 289–298, 2014.

[3] S. Mohammadzadeh bina, H. Fujii, S. Tsuya, H. Kosukegawa, S. Naganawa, and R. Harada, "Evaluation of utilizing horizontal directional drilling technology for ground source heat pumps," *Geothermics*, vol. 85, Article ID 101769, 2020.

[4] F. Wang, T. Ren, S. Tu, F. Hungerford, and N. Aziz, "Implementation of underground longhole directional drilling technology for greenhouse gas mitigation in Chinese coal mines," *International Journal of Greenhouse Gas Control*, vol. 11, pp. 290–303, 2012.

[5] X. Wang, D. Zhang, C. Zhao, P. Zhang, Y. Zhang, and Y. Cai, "Optimal design of lightweight serial robots by integrating

topology optimization and parametric system optimization," *Mechanism and Machine Theory*, vol. 132, pp. 48–65, 2019.

[6] D. Jasoliya, D. B. Shah, and A. M. Lakdawala, "Topological optimization of wheel assembly components for all terrain vehicles," *Materials Today Proceedings*, vol. 59, pp. 878–883, 2022.

[7] F. Di trapani, A. P. Sberna, and G. C. Marano, "A new genetic algorithm-based framework for optimized design of steel-jacketing retrofitting in shear-critical and ductility-critical RC frame structures," *Engineering Structures*, vol. 243, Article ID 112684, 2021.

[8] F. Di trapani, A. P. Sberna, and G. C. Marano, "A genetic algorithm-based framework for seismic retrofitting cost and expected annual loss optimization of non-conforming reinforced concrete frame structures," *Computers and Structures*, vol. 271, Article ID 106855, 2022.

[9] J. Xu, X. Gao, and D. Qu, "Multi-objective topology optimization for supporting plate of winch drum spindle," in *Proceedings of the International Conference on Mechanical Design*, pp. 389–402, Springer, Singapore, November 2018.

[10] D. Xiao, H. Zhang, X. Liu, T. He, and Y. Shan, "Novel steel wheel design based on multi-objective topology optimization," *Journal of Mechanical Science and Technology*, vol. 28, no. 3, pp. 1007–1016, 2014.

[11] Z. Sun, Y. Wang, Z. Gao, and Y. Luo, "Topology optimization of thin-walled structures with directional straight stiffeners," *Applied Mathematical Modelling*, vol. 113, pp. 640–663, 2023.

[12] C. Wu, C. Yang, Q. Xiao, H. Ke, and H. Xu, "Topology optimization of porous solid structures for heat transfer and flow channels in reactors with fluid-solid reaction coupling," *International Journal of Thermal Sciences*, vol. 181, Article ID 107771, 2022.

[13] X. Shao, Z. Chen, M. Fu, and L. Gao, "Multi-objective topology optimization of structures using nn-oc algorithms," in *Proceedings of the International Symposium on Neural Networks*, pp. 204–212, Springer, Berlin Heidelberg, 2007.

[14] G. Kazakis and N. D. Lagaros, "Topology optimization based material design for 3D domains using MATLAB," *Applied Sciences*, vol. 12, no. 21, Article ID 10902, 2022.

[15] G. Guo, Y. Zhao, and W. Zuo, "Explicit and efficient topology optimization for three-dimensional structures considering geometrical nonlinearity," *Advances in Engineering Software*, vol. 173, Article ID 103238, 2022.

[16] Z. Luo, L. Chen, J. Yang, Y. Zhang, and K. Abdel-Malek, "Compliant mechanism design using multi-objective topology optimization scheme of continuum structures," *Structural and Multidisciplinary Optimization*, vol. 30, no. 2, pp. 142–154, 2005.

[17] T. Iqbal, L. Wang, D. Li et al., "A general multi-objective topology optimization methodology developed for customized design of pelvic prostheses," *Medical Engineering and Physics*, vol. 69, pp. 8–16, 2019.

[18] H. Kristiansen, K. Poulios, and N. Aage, "Topology optimization for compliance and contact pressure distribution in structural problems with friction," *Computer Methods in Applied Mechanics and Engineering*, vol. 364, Article ID 112915, 2020.

[19] Y. Zhang, Y. Shan, X. Liu, and T. He, "An integrated multi-objective topology optimization method for automobile wheels made of lightweight materials," *Structural and Multidisciplinary Optimization*, vol. 64, no. 3, pp. 1585–1605, 2021.

[20] Y. Wang, S. Chen, and J. Tang, "A lightweight design method for aviation gear webs based on OptiStruct-ABAQUS [J]," *Mechanical transmission*, vol. 43, no. 7, pp. 60–65, 2019.

[21] Z. Zhang, C. Ren, Z. Xu, Y. S. He, and W. Li, "Research on multi-objective topology optimization of vehicle suspension control arm," *Journal of Mechanical Engineering*, vol. 53, no. 4, pp. 114–121, 2017.

[22] W. Zhong, R. Su, L. Gui, and Z. Fan, "Multi-objective topology and sizing optimization of bus body frame," *Structural and Multidisciplinary Optimization*, vol. 54, no. 3, pp. 701–714, 2016.

[23] Y. C. Chang, W. H. Lee, and C. H. Wu, "Airline new route selection using compromise programming - the case of Taiwan-Europe," *Journal of Air Transport Management*, vol. 76, pp. 10–20, 2019.

[24] M. Arenas parra, A. Bilbao terol, B. Pérez gladish, and M. Rodŕiguez Urŕia, "Solving a multiobjective possibilistic problem through compromise programming," *European Journal of Operational Research*, vol. 164, no. 3, pp. 748–759, 2005.

[25] F. Lan, F. Lai, J. Chen, and F. W. Ma, "Multi-case topology optimization of body structure considering dynamic characteristic," *Journal of Mechanical Engineering*, vol. 50, no. 20, pp. 122–128, 2014.

[26] D. Yu and X. Hong, "A theme evolution and knowledge trajectory study in AHP using science mapping and main path analysis," *Expert Systems with Applications*, vol. 205, Article ID 117675, 2022.

[27] Y. Xu, S. Liu, J. Wang, and X. Shang, "Consensus checking and improving methods for AHP with q-rung dual hesitant fuzzy preference relations," *Expert Systems with Applications*, vol. 208, Article ID 117902, 2022.

[28] N. Zhu, J. Liu, and X. Liu, "Multiobjective topology optimization of spatial-structure joints," *Advances in Civil Engineering*, vol. 2021, Article ID 5530644, 13 pages, 2021.

[29] R. Zhang, C. Gao, X. Chen, F. Li, D. Yi, and Y. Wu, "Genetic algorithm optimised Hadamard product method for inconsistency judgement matrix adjustment in AHP and automatic analysis system development," *Expert Systems with Applications*, vol. 211, Article ID 118689, 2023.

[30] C. Su and J. Xian, "Topology optimization of non-linear viscous dampers for energy-dissipating structures subjected to non-stationary random seismic excitation," *Structural and Multidisciplinary Optimization*, vol. 65, no. 7, p. 200, 2022.